33MeV and ETA Activation Analysis

Lawrence Berkeley National Laboratory, Berkeley, California 94720, USA
University of California, Berkeley, California 94720, USA
January, 2018

The Experiment

On April 25-27th 2017, a neutron activation experiment was performed at the 88-Inch Cyclotron located at Lawrence Berkeley National Lab. The purpose of the experiment was to determine how James Bevins' ETA design shifted the spectrum of fast neutrons produced by $33MeV$ deuterons on a tantalum breakup target. In order to determine how the ETA shifted the neutron spectrum, a suite of foils were irradiated and their gamma spectra measured to determine the activations of the foils by the beam. With these activations a spectrum unfold could be performed to determine the energy spectrum of the incident neutron beam.

The irradiation took place at LBNL's Deuteron-Breakup Neutron Facility shown in Figure 1. The 88-Inch Cyclotron was used to produce a $33MeV$ deuteron beam. Three foil packs were irradiated in the experiment. The first, foil pack #1, was used to determine experimental geometry and coincident summing correction factors for the other foil packs. The gamma spectra from this foil pack will be referred to as data set 1. With a beryllium breakup target placed in Cave 01 instead of the vault, foil pack #1 was irradiated for 16 minutes. Following irradiation, each of the foils in this pack was counted using a high purity germanium detector. They were counted $18cm$ from the detector, and over the next couple of days they were also counted $1cm$ from the detector.

With a tantalum breakup target in the vault, foil pack #2 was irradiated for two hours and twelve minutes with an average current around $8.5\mu A$. Following irradiation, each foil was counted $1cm$ from the detector. These gamma spectra are referred to as data set 2 and they were used to calculate the activation of each foil by the neutron beam without the ETA.

Keeping the breakup target setup, foil pack #3 was placed inside the ETA and irradiated for nineteen hours and thirty minutes with an average current of $12\mu A$. The gamma spectra from these foils were counted $1cm$ from the detector. These spectra are referred to as data set 3 and were used to calculate the activation of each foil after irradiation from inside the ETA.
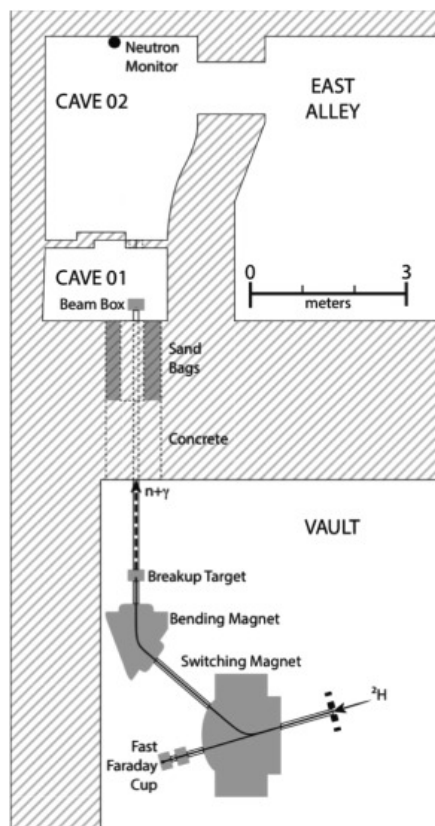

Figure 1: LBNL's Deuteron-Breakup Neutron Facility. Image courtesy of K.P. Harrig et al., Neutron Spectroscopy for pulsed beams with frame overlap using a double time-of-flight technique, (2018)

In order to perform the spectrum unfold, the following reaction channels were analyzed:

Reactions of Interest	
Reaction	Characteristic Gamma (keV)
Al-27, (n,p), Mg-27	1014.52
Al-27, (n,α), Na-24	1368.63
Au-197, (n,2n), Au-196	355.7
Au-197, (n,γ), Au-198	411.8
In-115, (n,n'), In-115m	336.241
In-115, (n,γ), In-116m	1293.56
Ni-58, (n,2n), Ni-57	1377.63
Ni-58, (n,p), Co-58	810.76
Zr-90, (n,2n), Zr-89	909.15

Energy Calibration

Radware's gf3 was used to analyze gamma spectra from a set of standard sources to construct an energy calibration curve. By fitting a gaussian to each of the peaks of interest, gf3 returned the channel number for that gamma peak as well as the total number of counts in the peak. Using these channel numbers and matching them to the expected energies, the energies were plotted as a function of channel number. Since each source measured had several energies that could be used for the calibration, there are 19 points used to construct the energy calibration curve. The standard sources used to construct the curve as well as their known gamma energies are listed in the table to the right.

At both 1 cm and 18 cm, a linear fit was used for the calibration. The results of the fit are given in the table below. The slope is reported in energy (keV) per channel number (CN). The uncertainties reported here are the standard error for the slope and the standard error of the y-intercept; a measure of the spread of the data points from the line.

Standards	
Source	Known Gamma Energy(keV)
^{241}Am	59.5409
^{133}Ba	80.9979
^{133}Ba	276.3989
^{133}Ba	302.8508
^{133}Ba	356.0129
^{60}Co	1173.228
^{60}Co	1332.492
^{137}Cs	661.657
^{152}Eu	121.7817
^{152}Eu	244.6974
^{152}Eu	344.2785
^{152}Eu	778.9045
^{152}Eu	964.057
^{152}Eu	1085.837
^{152}Eu	1112.076
^{152}Eu	1408.013
^{88}Y	392.87
^{88}Y	898.042
^{88}Y	1836.063

Calibration Results			
Distance (cm)	Slope (keV/CN)	y-intercept (keV)	R^2
1	0.39716 ± 0.00008	-0.3 ± 0.18	1.0000
18	0.39720 ± 0.00009	-0.4 ± 0.19	1.0000

Efficiency Calculation

The efficiency function was calculated using a least squares method. On physical grounds, the efficiency curves asymptotically approach a E_γ^{-1} relationship, so we do a linear least squares regression with the basis vectors x, 1, $\frac{1}{x}$, $\frac{1}{x^2}$ to fit the inverse efficiencies. The resulting function has a chi-square per degrees of freedom of 2.3 and is given by the following equation as a function of energy. The error bars displayed in Figure 2 are uncertainties in the current activities of each standard nuclide, calculated from the uncertainty in their initial activities.
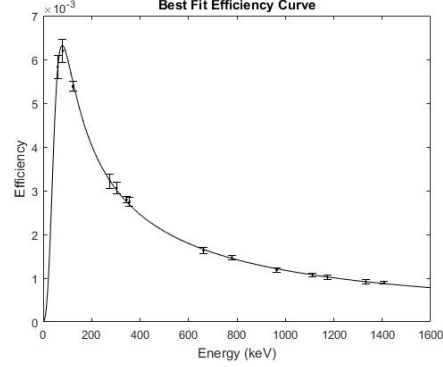

Figure 2: Efficiency at 18 cm

$$\epsilon_{18}(E_\gamma) = \frac{E_\gamma{}^2}{(0.7115)E_\gamma{}^3 + (147.8817)E_\gamma{}^2 - (1169.8)E_\gamma + 63775}$$

Initial Activity Equation

In order to perform a neutron spectrum unfold, the activity of each foil immediately following irradiation must be calculated. The relevant factors in the initial activity calculation are as follows:

A_0 = the initial activity of the source at creation
C = measured counts
I = intensity of that gamma
f_l = the detector live-time fraction
λ = the decay constant associated with that gamma
t_0 = the irradiation stop time
t_1 = the counting start time
t_2 = the counting stop time
$\Delta t_c = t_2 - t_1$ = the total count time
$\Delta t_j = t_1 - t_0$ = the time between the end of irradiation and the start of the counting
$\epsilon(E_\gamma)$ = the efficiency of the detector for a given line

The initial activity calculation is based on Equation (1) from the Status Report of Neutron Radiation Effects and Damage to Neutron Imaging System Equipment at Lawrence Livermore National Laboratory [1].

$$A_0 = \frac{C\lambda}{(1 - e^{-\lambda \Delta t_c})\epsilon(E_\gamma)f_l I_\gamma} \tag{1}$$

Equation (1) gives the activity of the sample at the beginning of the time of measurement. The goal is to calculate the initial activity of the sample immediately following irradiation. To account for decay between

---

[1] D.L. Bleuel et al., Status Report of Neutron Radiation Effects and Damage to Neutron Imaging System Equipment at Lawrence Livermore National Laboratory, 4 (2017)

irradiation and measurement, an extra decay factor is added to Equation (1) to produce the following equation.

$$A_0 = \frac{C\lambda e^{\lambda \Delta t_j}}{(1 - e^{-\lambda \Delta t_c})\epsilon_d(E_\gamma)f_l I_\gamma} \tag{2}$$

Recall that data set 2 is the set of gamma spectra from the foils that were irradiated directly by the neutron beam, and data set 3 is the set of gamma spectra from the foils that were irradiated from inside the ETA. Since data sets 2 and 3 were both measured at 1 cm, we want the efficiency at 1 cm, $\epsilon_1(E_\gamma)$. The absolute detection efficiency is dependent not only on the gamma energy detected, but on the reaction producing the gamma as well since some reactions produce gammas in cascade that are detected in coincidence. Additionally, it depends on the geometry of the source. The absolute efficiency was not directly measured due to differences in counting geometry from the point sources used for calibrations and the large foils used for measurement. The absolute efficiency can be expressed as

$$\epsilon_d(E_\gamma) = F_d(E_\gamma)G_d\mathscr{E}_d(E_\gamma) \tag{3}$$

where

$F_d(E_\gamma)$, is the peak summing correction factor for a given characteristic gamma ray of a given nuclide at that distance.,

G_d, the geometric correction factor to the efficiency. This is a solid angle correction that accounts for the source being a volume source instead of a point source,

$\mathscr{E}_d(E_\gamma)$, the intrinsic energy dependent efficiency of the detector at that distance for single gamma sources. This intrinsic detector efficiency is distance dependent because the path length of gammas traveling through the detector depends on the distance between the source and the detector.

Although the foils were counted 1 cm from the detector, it would be beneficial to express the initial activities in terms of the absolute efficiency 18 cm from the detector, $\epsilon_{18}(E_\gamma)$. At large source to detector distances the absolute efficiency is dominated by the $\mathscr{E}_d(E_\gamma)$ term, because $F_{18} \approx 1$ since there is little coincidence summing for sources far from the detector. Additionally, the analytic value for the geometric correction factor is $G_{18} = 0.987$ for Ω_{vol}/Ω_{pt} where Ω is the solid angle. This correction factor is close to 1 for these foils at 18 cm because at large distances from the detector, the foils are similar to a point source. In the final efficiency calculations, values of G_{18} modeled in MCNP were used. At 18 cm from the detector, the absolute efficiency is approximately only a function of the gamma energy, with a small correction factor. So by constructing an efficiency curve as a function of energy for standard sources at 18 cm, the absolute efficiency can be determined to an excellent approximation for any of the sources of interest in data sets 2 and 3. The following method was used to express the initial activity as a function of the efficiency at 18 cm.

If we want the activity of the reaction associated with the E_γ gamma for a given nuclide at a distance of 1 cm, then we first count it at both 1 cm and 18 cm and recognize the following:

$$A_0 = \frac{C_1\lambda e^{\lambda \Delta t_{j(1cm)}}}{(1 - e^{-\lambda \Delta t_{c(1cm)}})\epsilon_1(E_\gamma)f_l I_\gamma} \tag{4a}$$

$$A_0 = \frac{C_{18}\lambda e^{\lambda \Delta t_{j(18cm)}}}{(1 - e^{-\lambda \Delta t_{c(18cm)}})\epsilon_{18}(E_\gamma)f_l I_\gamma} \tag{4b}$$

$$\frac{C_1\lambda e^{\lambda \Delta t_{j(1cm)}}}{(1 - e^{-\lambda \Delta t_{c(1cm)}})\epsilon_1(E_\gamma)f_l I_\gamma} = \frac{C_{18}\lambda e^{\lambda \Delta t_{j(18cm)}}}{(1 - e^{-\lambda \Delta t_{c(18cm)}})\epsilon_{18}(E_\gamma)f_l I_\gamma} \tag{4c}$$

So

$$\frac{C_1}{C_{18}} = \frac{\epsilon_1(E_\gamma)}{\epsilon_{18}(E_\gamma)}\kappa \tag{5}$$

where

$$\kappa = \frac{e^{\lambda\Delta t_{j(18cm)}}\left(1 - e^{-\lambda\Delta t_{c(1cm)}}\right)}{e^{\lambda\Delta t_{j(1cm)}}\left(1 - e^{-\lambda\Delta t_{c(18cm)}}\right)}\frac{f_{l(1cm)}}{f_{l(18cm)}} = e^{\lambda(\Delta t_{j(18cm)} - \Delta t_{j(1cm)})}\frac{\left(1 - e^{-\lambda\Delta t_{c(1cm)}}\right)}{\left(1 - e^{-\lambda\Delta t_{c(18cm)}}\right)}\frac{f_{l(1cm)}}{f_{l(18cm)}} \tag{6}$$

We can get the total detector efficiency at 1 cm for each reaction channel by taking the ratios of the counts for that reaction from data set 1.

$$\epsilon_1(E_\gamma) = \frac{1}{\kappa}\frac{C_1(\text{Data Set 1})}{C_{18}(\text{Data Set 1})}\epsilon_{18}(E_\gamma) \tag{7}$$

Recall that $\epsilon_{18}(E_\gamma)$ was calculated using point sources with known activities. In order to use this efficiency for data sets 2 and 3, there needs to be a geometric correction factor G_{18} because the sources measured were disks with a circumference of about 50mm. Adding in this factor and plugging in, we have our final equation. This equation can be used to calculate the initial activity of a foil from either data set 2 (the beam only irradiation data) or data set 3 (the data from irradiation from within the ETA). Since it can be used for either of these data sets, the initial activity of a foil from either of these data sets will be referred to generally as $A_0(\text{Data Set x})$.

$$A_0(\text{Data Set x}) = \frac{C_1(\text{Data Set x})\lambda e^{\lambda\Delta t_j}}{(1 - e^{-\lambda\Delta t_c})\epsilon_{18}(E_\gamma)G_{18}f_l I_\gamma}\frac{C_{18}(\text{Data Set 1})}{C_1(\text{Data Set 1})}\kappa \tag{8}$$

where

$$\kappa = e^{\lambda(\Delta t_{j(18cm)} - \Delta t_{j(1cm)})}\frac{\left(1 - e^{-\lambda\Delta t_{c(1cm)}}\right)}{\left(1 - e^{-\lambda\Delta t_{c(18cm)}}\right)}\frac{f_{l(1cm)}}{f_{l(18cm)}} \tag{9}$$

Results

By the time ^{27}Al and ^{115}In were measured at 1 cm, the $843.76keV$ energy for the Al1a foil and the $1293.56keV$ energy for the In1 foil had decayed away. Since Data Sets 2 and 3 needed efficiency ratio data for ^{27}Al(n,p)^{27}Mg reaction, the method used to approximate the initial activity was to analyze the $1014.52keV$ gamma peak for this reaction, and to use data from the ^{115}In(n,n')^{115m}In to calculate the correction factor $\frac{C_{18}(\text{Data Set 1})}{C_1(\text{Data Set 1})}\kappa$ for this peak since neither this $1014.52keV$ from ^{27}Mg nor the $336.24keV$ peak from ^{115m}In experience significant coincidence summing. The high purity aluminum was used to calculate the initial activity for the ^{27}Al$(n,a)^{24}$Na reaction, but note that the second count for Al1a (Row 5, Data Set 1) at 18 cm was used to calculate this.

Equations 8 and 9 were used to determine the initial activities of each reaction of interest. These results were then used to perform a spectrum unfold using STAYSL PNNL. It is important to note however, that the activities calculated this way do not account for gamma self-shielding. This is fine for activities being used as input for STAYSL PNNL as the software already accounts for gamma self-shielding. However, in order to compare the measured foil activities with the simulated activities, the activities including the gamma self-shielding factor are included in following tables.

33MeV Beam Only (no gamma self-shielding factor)				
Foil	Reaction	Gamma (keV)	Initial Activity (Bq)	Number of Atoms Activated
^{27}Al	^{27}Al(n,p)^{27}Mg	1014.52	1727 ± 69[1]	1414000 ± 57000[1]
^{27}Al	^{27}Al(n,a)^{24}Na	1368.63	225.5 ± 4.6	17510000 ± 360000
^{197}Au	^{197}Au(n,2n)^{196}Au	355.7	34.79 ± 1.65	26800000 ± 1270000
^{197}Au	^{197}Au(n,γ)^{198}Au	411.8	21.80 ± 1.06	7321000 ± 356000
^{115}In	^{115}In(n,n')^{115m}In	336.241	1709 ± 25	39830000 ± 580000
^{115}In	^{115}In(n,γ)^{116m}In	1293.56	5311 ± 97	24960000 ± 450000
^{58}Ni	^{58}Ni(n,2n)^{57}Ni	1377.63	17.31 ± 0.39	3201000 ± 72000
^{58}Ni	^{58}Ni(n,p)^{58}Co	810.76	9.283 ± 0.172	81990000 ± 1520000
^{90}Zr	^{90}Zr(n,2n)^{89}Zr	909.15	55.50 ± 1.05	22600000 ± 430000

Activations in ETA (no gamma self-shielding factor)				
Foil	Reaction	Gamma (keV)	Initial Activity (Bq)	Number of Atoms Activated
^{27}Al	^{27}Al(n,p)^{27}Mg	1014.52	410.1 ± 21.9[1]	381700 ± 17900[1]
^{27}Al	^{27}Al(n,a)^{24}Na	1368.63	387.7 ± 7.2	30130000 ± 560000
^{197}Au	^{197}Au(n,2n)^{196}Au	355.7	99.06 ± 4.70	76310000 ± 3620000
^{197}Au	^{197}Au(n,γ)^{198}Au	411.8	166.9 ± 4.7	56040000 ± 2690000
^{115}In	^{115}In(n,n')^{115m}In	336.241	2801 ± 43	65270000 ± 1000000
^{115}In	^{115}In(n,γ)^{116m}In	1293.56	5548 ± 113	26070000 ± 530000
^{58}Ni	^{58}Ni(n,2n)^{57}Ni	1377.63	42.49 ± 0.88	7855000 ± 162000
^{58}Ni	^{58}Ni(n,p)^{58}Co	810.76	28.05 ± 0.50	247800000 ± 4400000
^{90}Zr	^{90}Zr(n,2n)^{89}Zr	909.15	143.4 ± 2.7	58410000 ± 1100000

The following activities were all calculated including the gamma self-shielding factor. These should not be used as inputs to STAYSL PNNL.

33MeV Beam Only (with gamma self-shielding factor)					
Foil	Reaction	Gamma (keV)	Initial Activity (Bq)	Sim Init Act (Bq)	Number of Atoms Activated
^{27}Al	^{27}Al(n,p)^{27}Mg	1014.52	1741 ± 70[1]	1098[2]	1425000 ± 57000[1]
^{27}Al	^{27}Al(n,a)^{24}Na	1368.63	227.0 ± 4.6	218	17630000 ± 360000
^{197}Au	^{197}Au(n,2n)^{196}Au	355.7	35.66 ± 1.69	23.9	27470000 ± 1300000
^{197}Au	^{197}Au(n,γ)^{198}Au	411.8	22.22 ± 1.08	0.7[3]	7461000 ± 363000
^{115}In	^{115}In(n,n')^{115m}In	336.241	1801 ± 26	622[3]	41970000 ± 610000
^{115}In	^{115}In(n,γ)^{116m}In	1293.56	5411 ± 98	209[3]	25430000 ± 460000
^{58}Ni	^{58}Ni(n,2n)^{57}Ni	1377.63	17.72 ± 0.40	17.7	3276000 ± 73000
^{58}Ni	^{58}Ni(n,p)^{58}Co	810.76	9.283 ± 0.172	15.3[4]	81990000 ± 1520000
^{90}Zr	^{90}Zr(n,2n)^{89}Zr	909.15	55.50 ± 1.05	64.7[4]	22600000 ± 430000

Activations in ETA (with gamma self-shielding factor)				
Foil	Reaction	Gamma (keV)	Initial Activity (Bq)	Number of Atoms Activated
^{27}Al	^{27}Al(n,p)^{27}Mg	1014.52	413.5 ± 22.1[1]	338500 ± 18100[1]
^{27}Al	^{27}Al(n,a)^{24}Na	1368.63	390.5 ± 7.3	30340000 ± 570000
^{197}Au	^{197}Au(n,2n)^{196}Au	355.7	101.5 ± 4.8	78200000 ± 3710000
^{197}Au	^{197}Au(n,γ)^{198}Au	411.8	170.0 ± 8.2	57100000 ± 2740000
^{115}In	^{115}In(n,n')^{115m}In	336.241	2951 ± 45	68760000 ± 1050000
^{115}In	^{115}In(n,γ)^{116m}In	1293.56	5653 ± 115	26570000 ± 540000
^{58}Ni	^{58}Ni(n,2n)^{57}Ni	1377.63	43.48 ± 0.90	8040000 ± 170000
^{58}Ni	^{58}Ni(n,p)^{58}Co	810.76	28.05 ± 0.50	247800000 ± 4400000
^{90}Zr	^{90}Zr(n,2n)^{89}Zr	909.15	143.4 ± 2.7	58410000 ± 1100000

[1]These values determined using data from ^{115}In(n,n')^{115m}In reaction as a reference.

[2] This value should be modeled well, so the discrepancy should be investigated.

[3] These channels will be underpredicted in the model due to use of Meulder's as a starting source (no neutrons < 2 MeV).

[4] These channels are also fed from other reactions on other isotopes in natural Ni/Zr. Therefore, we'd expect the model to underpredict these channels, but the opposite happened.

Uncertainty Propagation

An approximate uncertainty in the initial activities was calculated using propagation of uncertainty. The uncertainty is given by

$$(\sigma_{A_0})^2 = \left(\frac{\partial A_0}{\partial C_1(x)}\right)^2 (\sigma_{C_1(x)})^2 + \left(\frac{\partial A_0}{\partial \Delta t_j}\right)^2 (\sigma_{\Delta t_j})^2 + \left(\frac{\partial A_0}{\partial C_{18}(1)}\right)^2 (\sigma_{C_{18}(1)})^2 + \left(\frac{\partial A_0}{\partial \kappa}\right)^2 (\sigma_\kappa)^2$$

$$+ \left(\frac{\partial A_0}{\partial \Delta t_c}\right)^2 (\sigma_{\Delta t_c})^2 + \left(\frac{\partial A_0}{\partial \epsilon_{18}}\right)^2 (\sigma_{\epsilon_{18}})^2 + \left(\frac{\partial A_0}{\partial F_{18}}\right)^2 (\sigma_{F_{18}})^2 + \left(\frac{\partial A_0}{\partial C_1(1)}\right)^2 (\sigma_{C_1(1)})^2$$

where

$$(\sigma_\kappa)^2 = \left(\frac{\partial \kappa}{\partial \Delta t_{j(18)}}\right)^2 (\sigma_{\Delta t_{j(18)}})^2 + \left(\frac{\partial \kappa}{\partial \Delta t_{j(1)}}\right)^2 (\sigma_{\Delta t_{j(1)}})^2 + \left(\frac{\partial \kappa}{\partial \Delta t_{c(18)}}\right)^2 (\sigma_{\Delta t_{c(18)}})^2 + \left(\frac{\partial \kappa}{\partial \Delta t_{c(1)}}\right)^2 (\sigma_{\Delta t_{c(1)}})^2$$

This error equation becomes

$$(\sigma_{A_0})^2 = \left(\frac{A_0}{C_1(x)}\right)^2 (\sigma_{C_1(x)})^2 + (A_0\lambda)^2(\sigma_{\Delta t_j})^2 + \left(\frac{A_0}{C_{18}(1)}\right)^2 (\sigma_{C_{18}(1)})^2 + \left(\frac{A_0}{\kappa}\right)^2 (\sigma_\kappa)^2$$

$$+ \left(\frac{A_0\lambda e^{-\lambda \Delta t_c}}{1 - e^{-\lambda \Delta t_c}}\right)^2 (\sigma_{\Delta t_c})^2 + \left(\frac{A_0}{\epsilon_{18}}\right)^2 (\sigma_{\epsilon_{18}})^2 + \left(\frac{A_0}{F_{18}}\right)^2 (\sigma_{F_{18}})^2 + \left(\frac{A_0}{C_1(1)}\right)^2 (\sigma_{C_1(1)})^2$$

where

$$(\sigma_\kappa)^2 = (\kappa\lambda)^2 (\sigma_{\Delta t_{j(18)}})^2 + (\kappa\lambda)^2(\sigma_{\Delta t_{j(1)}})^2 + \left(\frac{\kappa\lambda e^{-\Delta t_{c(18)}}}{1 - e^{-\Delta t_{c(18)}}}\right)^2 (\sigma_{\Delta t_{c(18)}})^2 + \left(\frac{\kappa\lambda e^{-\Delta t_{c(1)}}}{1 - e^{-\Delta t_{c(1)}}}\right)^2 (\sigma_{\Delta t_{c(1)}})^2$$

This becomes

$$(\sigma_{A_0})^2 = (A_0)^2 \left[\left(\frac{1}{C_1(x)}\right)^2 (\sigma_{C_1(x)})^2 + (\lambda)^2(\sigma_{\Delta t_j})^2 + \left(\frac{1}{C_{18}(1)}\right)^2 (\sigma_{C_{18}(1)})^2 + \left(\frac{1}{\kappa}\right)^2 (\sigma_\kappa)^2\right]$$

$$+ (A_0)^2 \left[\left(\frac{\lambda e^{-\lambda \Delta t_c}}{1 - e^{-\lambda \Delta t_c}}\right)^2 (\sigma_{\Delta t_c})^2 + \left(\frac{1}{\epsilon_{18}}\right)^2 (\sigma_{\epsilon_{18}})^2 + \left(\frac{1}{F_{18}}\right)^2 (\sigma_{F_{18}})^2 + \left(\frac{1}{C_1(1)}\right)^2 (\sigma_{C_1(1)})^2\right]$$

where

$$(\sigma_\kappa)^2 = (\kappa\lambda)^2 \left[(\sigma_{\Delta t_{j(18)}})^2 + (\sigma_{\Delta t_{j(1)}})^2 + \left(\frac{e^{-\Delta t_{c(18)}}}{1 - e^{-\Delta t_{c(18)}}}\right)^2 (\sigma_{\Delta t_{c(18)}})^2 + \left(\frac{e^{-\Delta t_{c(1)}}}{1 - e^{-\Delta t_{c(1)}}}\right)^2 (\sigma_{\Delta t_{c(1)}})^2\right]$$

All the time measurements have an uncertainty of half a second. Any Δt term consists of two time measurements subtracted from each other. So the uncertainty on any Δt term will be given by the following

$$\sigma_{\Delta t} = \sqrt{(0.5)^2 + (0.5)^2} = \sqrt{0.5}$$

$$(\sigma_{\Delta t})^2 = 0.5$$

So the error is finally

$$(\sigma_{A_0})^2 = (A_0)^2 \left[\left(\frac{1}{C_1(x)} \right)^2 (\sigma_{C_1(x)})^2 + 0.5(\lambda)^2 + \left(\frac{1}{C_{18}(1)} \right)^2 (\sigma_{C_{18}(1)})^2 + \left(\frac{1}{\kappa} \right)^2 (\sigma_\kappa)^2 \right]$$

$$+ (A_0)^2 \left[0.5 \left(\frac{\lambda e^{-\lambda \Delta t_c}}{1 - e^{-\lambda \Delta t_c}} \right)^2 + \left(\frac{1}{\epsilon_{18}} \right)^2 (\sigma_{\epsilon_{18}})^2 + \left(\frac{1}{F_{18}} \right)^2 (\sigma_{F_{18}})^2 + \left(\frac{1}{C_1(1)} \right)^2 (\sigma_{C_1(1)})^2 \right]$$

where

$$(\sigma_\kappa)^2 = (\kappa \lambda)^2 \left[1 + 0.5 \left(\frac{e^{-\Delta t_{c(18)}}}{1 - e^{-\Delta t_{c(18)}}} \right)^2 + 0.5 \left(\frac{e^{-\Delta t_{c(1)}}}{1 - e^{-\Delta t_{c(1)}}} \right)^2 \right]$$

The uncertainty in the efficiencies will be dominated by the uncertainties in the activities of the sources used to construct the efficiency curve. None of these uncertainties are greater than 1.2% so this value was used as an upper bound for the uncertainty in the efficiency.

Integrated Fluence

The integrated fluence equation comes from Equation (2) of the Status Report of Neutron Radiation Effects and Damage to Neutron Imaging System Equipment at Lawrence Livermore National Laboratory [2].

$$\Psi_{foil} = \frac{A_0 A_{Al}}{m_{Al} N_A \langle \sigma \rangle} \frac{\sum_i \frac{I_i}{I_0} \Delta t_i}{\sum_i \frac{I_i}{I_0} (1 - e^{-\lambda \Delta t_i}) e^{-\lambda \Delta t_{dk,i}}} \tag{10}$$

$$\Psi_{foil} = \frac{A_0 A_{Al}}{m_{Al} N_A \langle \sigma \rangle} \frac{\Delta t}{(1 - e^{-\lambda \Delta t}) e^{-\lambda \Delta t_{dk}}} \tag{11}$$

where

$$\langle \sigma \rangle = \frac{\int_E \frac{d\Phi}{dE} \sigma dE}{\int_E \frac{d\Phi}{dE} dE} \tag{12}$$

The equation above takes the initial activities as the activities at the start of counting. Since the initial activities we have are the activities at the end of irradiation, we can drop the factor of $e^{-\lambda \Delta t_{dk}}$. So the equation used to calculate the integrated fluence here is

$$\Psi_{foil} = \frac{A_0 A_{Al}}{m_{Al} N_A \langle \sigma \rangle} \frac{\Delta t}{(1 - e^{-\lambda \Delta t})} \tag{13}$$

where $\langle \sigma \rangle$ is located in the STAYSL output for each reaction.
For the Al27(n,a)Na24 reaction, the calculation is modeled below:

$$\Psi_{foil} = \frac{390 Bq * 27 Amu}{(5.284g)(6.022 \times 10^{23})(1.2004 \times 10^{-26} cm^2/neutron)} \frac{(70200s)}{(1 - e^{-(1.287 \times 10^{-5} s^{-1}) 70200 s})} \tag{14}$$

$$\Psi_{foil} = 3.253 \times 10^{10} neutrons/cm^2 \tag{15}$$

---

[2]D.L. Bleuel et al., Status Report of Neutron Radiation Effects and Damage to Neutron Imaging System Equipment at Lawrence Livermore National Laboratory, 4 (2017)